ALTEX, accepted manuscript
published July 16, 2021
doi:10.14573/altex.2103311

Research Article

A New Approach Methodology (NAM) for the Prediction of (Nor)ibogaine-Induced Cardiotoxicity in Humans

Miaoying Shi, Sebastiaan Wesseling, Hans Bouwmeester and Ivonne M. C. M. Rietjens
Division of Toxicology, Wageningen University and Research, Wageningen, The Netherlands

Abstract
The development of non-animal based New Approach Methodologies (NAMs) for chemical risk assessment and safety evaluation is urgently needed. The aim of the present study was to investigate the applicability of an *in vitro in silico* approach to predict human cardiotoxicity of the herbal alkaloid ibogaine and its metabolite noribogaine, being promising anti-addiction drugs. Physiologically based kinetic (PBK) models were developed using *in silico*-derived parameters and biokinetic data obtained from *in vitro* liver microsomal incubations and Caco-2 transport studies. Human induced pluripotent stem cell-derived cardiomyocytes combined with the multi-electrode array (MEA) assay were used to determine *in vitro* concentration-dependent cardiotoxicity reflected by prolongation of field potential duration, which was subsequently translated to *in vivo* dose-dependent prolongation of the QTc (heart rate corrected time duration from ventricular depolarization to repolarization) using PBK model based reverse dosimetry. Results showed that the predictions matched well with available *in vivo* kinetic data and QTc data for ibogaine and noribogaine available in literature, indicating a good performance of the NAM. Benchmark dose analysis of the predicted dose response curves adequately predicted the onset of *in vivo* cardiotoxicity detected by QTc prolongation upon oral exposure to ibogaine and noribogaine. The present study provides an additional proof of principle of using PBK modeling-based reverse dosimetry as a NAM to predict human cardiotoxicity.

1 Introduction

In line with the 3Rs principle, the development of non-animal based novel methods has been a leading research topic towards New Approach Methodologies (NAMs) for chemical risk assessment and safety evaluation (Andersen et al., 2019; ICCVAM, 2018; Taboureau et al., 2020).The NAMs using *in vitro* and *in silico* models have become increasingly important for predicting human toxicity as they are high throughput in generating data and reduce animal use and costs (Bos et al., 2020; Patterson et al., 2020). Within the frame of NAMs, the biological effects of chemicals are characterized by *in vitro* toxicity assays with target organ specificity and reflecting the relevant mode of action, while the biokinetics related to absorption, distribution, metabolism and distribution (ADME) can be captured by using *in vitro* and/or computational models (Andersen et al., 2019; Punt et al., 2020). One good example of such NAMs is so-called physiologically based kinetic (PBK) modelling-based reverse dosimetry, which has been shown to be of use for quantitative *in vitro in vivo* extrapolation (QIVIVE) enabling definition of *in vivo* dose response curves for different toxic endpoints (Abdullah et al., 2016; Gilbert-Sandoval et al., 2020; Louisse et al., 2010; Rietjens et al., 2011; Strikwold et al., 2017; Zhao et al., 2019), including cardiotoxicity (Shi et al., 2020a).

In our previous work, we demonstrated that *in vivo* methadone-induced QTc prolongation (heart rate corrected time duration from ventricular depolarization to repolarization) can be adequately predicted based on *in vitro* cardiotoxic effects of methadone on human induced pluripotent stem cell-derived cardiomyocytes (hiPSC-CMs) combined with PBK modelling (Shi et al., 2020a). Given that cardiotoxicity is one of the most common toxic endpoints and a main concern for discontinuing drug development (Ovics et al., 2020; Pang et al., 2019), it is of importance to validate the applicability and accuracy of this newly developed NAM by providing additional proofs of principle for the evaluation of cardiotoxicity. Thus, the aim of the present study was to apply the developed PBK modelling-based reverse dosimetry approach to predict the cardiotoxicity of ibogaine and its metabolites, which are plant-based substances that attracted special attention due to their potential cardiotoxicity occurring in the clinical setting (Schep et al., 2016).

Received March 31, 2021; Accepted July 5, 2021;
Epub July 16, 2021; © The Authors, 2021.

ALTEX 38(#), ###-###. doi:10.14573/altex.2103311

Correspondence: Miaoying Shi
Division of Toxicology, Wageningen University
Stippeneng 4, 6708 WE Wageningen, the Netherlands
(miaoying.shi@wur.nl)

ALTEX, accepted manuscript
published July 16, 2021
doi:10.14573/altex.2103311

Ibogaine is an indole alkaloid naturally occurring in the West African shrub *Tabernanthe iboga*, which was traditionally used for medical treatment and religious ceremonies (Davis et al., 2017; Goutarel et al., 1993; Litjens and Brunt, 2016; Mash et al., 2018). Nowadays ibogaine is banned or allowed only under medical supervision in most countries due to its psychoactive properties with the exception of New Zealand (Noller et al., 2018). It is used given that a single high dose of ibogaine can be effective for reducing drug-induced withdrawal symptoms in human (Alper et al., 1999; Mash et al., 2018; Noller et al., 2018). Ibogaine is mainly metabolized by the hepatic cytochromes P450 (CYPs) via *O*-demethylation to the primary metabolite noribogaine, which is also psychoactive and has pharmacological effects (Obach et al., 1998; Glue et al., 2016; Mash et al., 2016; Litjens and Brunt, 2016). The major enzyme involved in the conversion of ibogaine to noribogaine has been identified in both *in vitro* and *in vivo* studies to be CYP2D6 (Obach et al., 1998; Glue et al., 2015b), with minor contributions from CYP2C9 and CYP3A4 (Obach et al., 1998). Subsequently, noribogaine is cleared via glucuronidation to noribogaine glucuronide (Glue et al., 2015a,b, 2016) (Figure 1).

The efficacy and safety of ibogaine and noribogaine for the treatment of drug addiction has been under debate over decades. Despite evidence obtained in preclinical and clinical studies showing promising pharmacological efficacy, cardiotoxicity was identified as the major safety concern for its clinical use (Schep et al., 2016). Several fatalities and case reports described patients who received a high dose of ibogaine after which they experienced prolonged QTc interval, which could further develop to cardiac arrythmia and even sudden death (Asua, 2013; Grogan et al., 2019; Hildyard et al., 2016; Hoelen et al., 2009; O'Connell et al., 2015; Paling et al., 2012; Pleskovic et al., 2012; Steinberg and Deyell, 2018; Vlaanderen et al., 2014). Furthermore, Glue et al. (2016) observed a dose-dependent effect of noribogaine on QTc prolongation in opioid-dependent patients. The observed QT prolongation could be associated with the potential inhibitory effect of both compounds on human ether-à-go-go-related gene (hERG) channels that play a critical role in cardiac repolarization (Martin et al., 2004). Based on *in vitro* studies using the electrophysiological-based patch clamp technique, both ibogaine and noribogaine were reported to block the hERG channels with similar potency (Alper et al., 2016; Koenig et al., 2014; Rubi et al., 2017).

In the present study, to predict the cardiotoxicity upon oral exposure to ibogaine or noribogaine using PBK model based reverse dosimetry, the *in vitro* cardiotoxicity of the two compounds was quantified in hiPSC-CMs using the multiple-electrode array (MEA) technique. The obtained data were subsequently combined with *in vitro* biokinetic data and used in a PBK model based reverse dosimetry approach to predict human dose-response curves. The hiPSC-CM MEA assay quantifies the extracellular field potential duration corrected for beat rate (FPDc) as an *in vitro* surrogate of QTc prolongation in the human electrocardiogram (ECG). The biokinetic data describing absorption and metabolism of ibogaine and noribogaine, obtained from *in vitro* experiments, were integrated in a PBK model for ibogaine with a submodel for noribogaine in human. Subsequently the PBK model was used to translate the *in vitro* concentration-dependent cardiotoxicity to the predicted dose-dependent cardiotoxic effects on QTc prolongation in human. The obtained data were compared to reported human *in vivo* data on ibogaine and noribogaine-induced QTc prolongation. Benchmark dose (BMD) analysis of the predicted *in vivo* dose-response curves was performed to allow comparison to available data on human cardiotoxicity and validate the predictions. From the predicted dose-response curve, points of departure (PoDs) can be derived to define a safe level of exposure and to evaluate the risk by comparing the PoD values with exposure levels, thus providing insight in the use of the NAM to evaluate the risk of ibogaine and noribogaine-induced cardiotoxicity in the clinical setting.

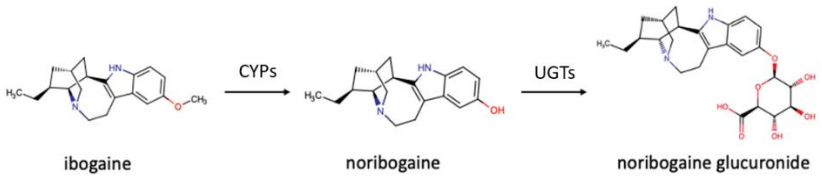

Fig: 1: Metabolic pathway of ibogaine to noribogaine by cytochromes P450 (CYPs) and subsequent conversion of noribogaine to noribogaine glucuronide by glucuronosyltransferases (UGTs)

2 Materials and methods[1]

2.1. Chemicals and biological materials

Ibogaine hydrochloride (99.5%), noribogaine hydrochloride (98.8%) and noribogaine glucuronide lithium salt (97.4%) were purchased from TLC Pharmaceutical Standards Ltd. (Newmarket, Ontario, Canada,). Antipyrine (≥ 99%), bovine serum albumin (BSA, ≥ 96%), dofetilide (≥ 98%), fibronectin, fluorescein (95%), isoproterenol hydrochloride (≥ 98%), methadone hydrochloride (≥ 98%), methanesulfonic acid (≥ 99%) and Tris (hydroxymethyl) aminomethane (Tris), were purchased from Sigma-Aldrich (Zwijndrecht, The Netherlands). Methadone was used under the opium exemption license number 104783 03 WCO, registered at Farmatec (executive organization of the Ministry of Health, Welfare and Sport, The Hague, The Netherlands). Dimethyl sulfoxide

[1] **Abbreviations:** ADME, absorption, distribution, metabolism and distribution; BMC, benchmark concentration; BMCL10, lower 95% confidence limit of the benchmark concentration resulting in 10% effect above background; BMD, benchmark dose; BMDL10, lower 95% confidence limit of the BMD resulting in 10% effect above background; CYP, cytochrome P450; ECG, electrocardiogram; FPDc, field potential duration corrected for beat rate; hERG, human ether-à-go-go-related gene; hiPSC-CM, human induced pluripotent stem cell-derived cardiomyocytes; MEA, multi-electrode array; NAM, new approach methodology; QIVIVE, quantitative in vitro in vivo extrapolation.

(DMSO, 99.7%) and sodium hydrogen carbonate ($NaHCO_3$, ≥ 99%) were obtained from Merck (Schiphol-Rijk, The Netherlands). Acetonitrile (UPLC/MS grade) was obtained from Biosolve BV (Valkenswaard, The Netherlands). Formic acid (FA) was purchased from VWR International (Amsterdam, The Netherlands).

hiPSC-CM (Pluricyte ® Cardiomyocytes, cat# PCMI-1031-1) and Pluricyte ® Cardiomyocyte medium were purchased from Ncardia (Leiden, The Netherlands). The human colon carcinoma cell line Caco-2 was obtained from ATCC (Manassas, VA, USA). Dulbecco's modified Eagle's medium (DMEM, GlutaMAX™ containing 4.5 g/L D-glucose and pyruvate), Hank's balanced salt solution (HBSS) without phenol red and phosphate-buffered saline (PBS) were obtained from Gibco (Paisley, Scotland, UK). Non-essential amino acids (NEAA) and penicillin-streptomycin (P/S) were purchased from Gibco (Grand Island, New York, USA). Fetal Bovine Serum (FBS) was purchased from Bodinco BV (Alkmaar, The Netherlands). Pooled human liver microsomes (Corning® UltraPool™ HLM 150, pooled from 150 donors with mixed gender), reduced nicotinamide adenine dinucleotide phosphate (NADPH) regenerating system solution A and solution B, glucuronosyltransferase (UGT) reaction mix system solution A and solution B were purchased from Corning (Woburn, MA, USA). Pooled human plasma and rapid equilibrium dialysis (RED) materials, including RED inserts, RED base plates and sealing tape were obtained from Thermo Fisher Scientific (Bleiswijk, The Netherlands).

2.2. General outline of the PBK modeling-based reverse dosimetry approach

The PBK modeling-based reverse dosimetry approach to predict the *in vivo* dose–response curves from *in vitro* cardiotoxicity concentration–response data included the following steps: i) establishment of the *in vitro* concentration–response curves for ibogaine and its metabolites noribogaine in hiPSC-CM using the MEA, ii) development of a PBK model for ibogaine and noribogaine in human using biokinetic data obtained from *in vitro* liver microsomal incubations and Caco-2 transport studies, and parameters derived from *in silico* simulations and the literature, iii) evaluation of the PBK model, iv) translation of *in vitro* concentration–response curves to *in vivo* dose–response curves using the PBK model, and v) evaluation of the PBK modeling-based reverse dosimetry approach by comparing predicted dose–response data to data obtained from literature on the effects of ibogaine and noribogaine on QTc prolongation. The general outline of the PBK modelling-based reverse dosimetry approach was illustrated in Figure 2.

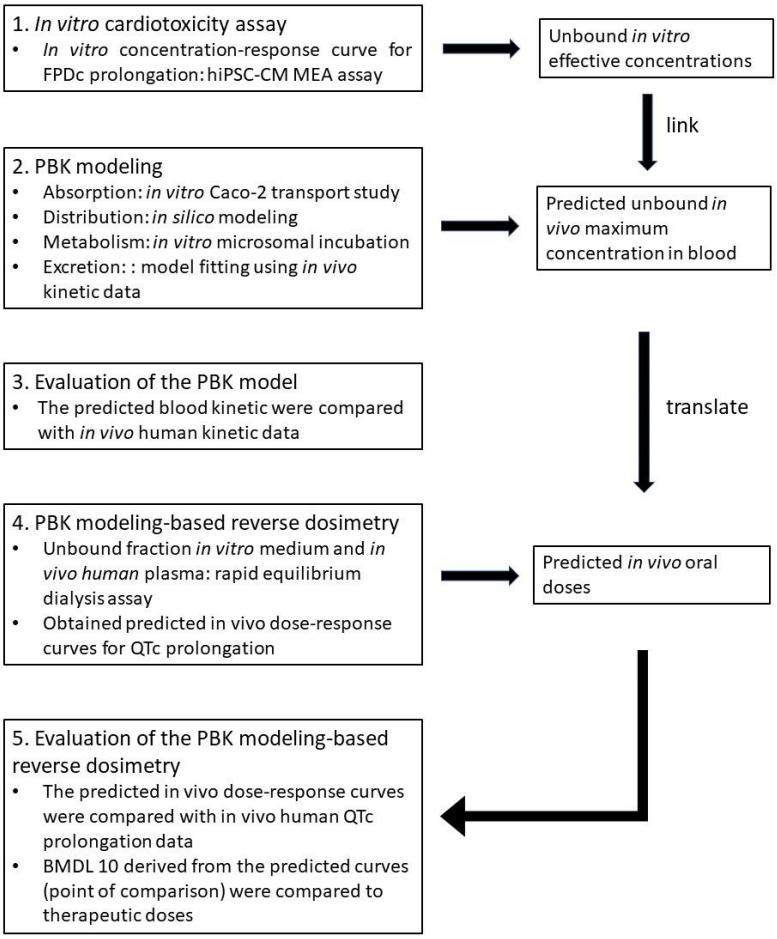

Fig. 2: General outline of the PBK modeling-based reverse dosimetry approach

$BMCL_{10}$, lower 95% confidence limit of the benchmark concentration resulting in 10% effect above background; FPDc, field potential duration corrected for beat rate; hiPSC-CM, human induced pluripotent stem cell-derived cardiomyocytes; MEA, multi-electrode array; PBK, physiologically based kinetic; QTc, (heart rate corrected time duration from ventricular depolarization to repolarization).

2.3. *In vitro* cardiotoxicity of ibogaine and noribogaine in the hiPSC-CM MEA assay

2.3.1 Exposure and MEA recording

The exposure and the recording of spontaneous beating of hiPSC-CMs were conducted as previously described (Shi et al., 2020a). Stock solutions of ibogaine were prepared in acetonitrile/water (50/50 v/v). Noribogaine and two references, dofetilide and isoproterenol, were dissolved in DMSO. All stock solutions were diluted in culture medium to make exposure medium with the final concentration of 0.05%(v/v) acetonitrile or 0.1% (v/v) DMSO. Based on cytotoxicity and relevant human plasma concentrations observed upon oral administration of ibogaine and noribogaine, the following concentrations were tested, 0 (control), 0.03, 0.1, 0.2, 0.3, 0.4, 0.5, 1 µM (ibogaine) and 0 (control), 0.03, 0.1, 0.2, 0.3, 0.4, 1, 3 µM (noribogaine). The test concentrations were 0 (control), 0.1, 0.3, 1, 3, 10 nM for dofetilide and 0 (control), 3, 10, 30, 100, 300 nM for isoproterenol, which are typical responsive concentrations in the hiPSC-CM MEA assay (Zwartsen et al. 2019).

The precoating of MEA chips (60-6well MEA200/30iR-Ti-tcr, MCS GmbH, Ruetlingen, Germany) and the culturing of Pluricyte® Cardiomyocytes (Ncardia) were prepared according to the manufacturer's protocol as previously described in Shi et al. (2020a). At day 7-9 post-seeding, extracellular field potentials of cardiomyocytes (Figure 3) were accessed by using the MEA2100-system (MCS GmbH) equipped with a chamber and a heating controller that guaranteed a stable atmosphere (37 °C with 5% CO_2). A 20 min equilibration period was applied prior to the compound/ vehicle exposure. Measurements started with replacing half of the medium in each well by fresh medium containing 0.1% (v/v) acetonitrile or 0.2%(v/v) DMSO to reach a final concentration of 0.05% (v/v) acetonitrile or 0.1% (v/v) DMSO, which was defined as baseline condition. Following the same way, each concentration of the model compounds was cumulatively added to the well increasing the concentration at each subsequent addition (Ando et al., 2017; Nozaki et al., 2017). In each MEA chip, five of the six wells were exposed to model or reference compounds while one well served as the vehicle control analyzed during a similar period of time as the other wells to enable corrections for time-, addition- and vehicle-dependent effects on the field potentials. At each concentration, exposure was conducted for 15 min followed by a 2 min recording of extracellular field potentials. Data were recorded using Cardio 2D software Version 2.12.0 (MCS GmbH) with a sample frequency of 10 kHZ and a 0.1–3.5 kHz band-pass filter.

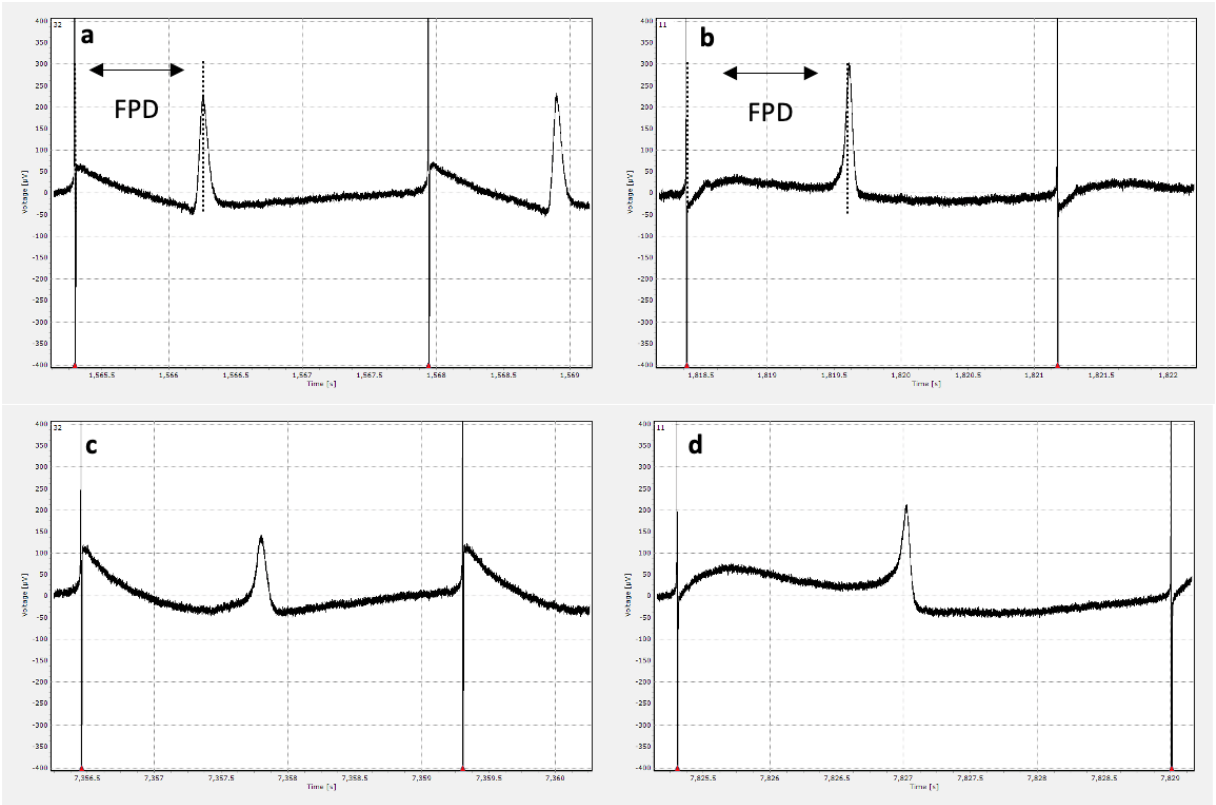

Fig. 3: Normal and prolonged waveforms of field potential observed in human induced pluripotent stem cell-derived cardiomyocytes using the multiple-electrode array

a, field potential duration (FPD) at baseline condition with the treatment of 0.05% (v/v) acetonitrile. b, FPD at baseline condition with the treatment of 0.1% (v/v) DMSO. c, prolonged FPD observed at 0.4 µM ibogaine. d, prolonged FPD observed at 0.4 µM noribogaine.

2.3.2 Data analysis and statistics

Raw data obtained from the hiPSC-CM MEA assay was analyzed using MultiwellAnalyzer software Version 1.8.6.0 (MCS GmbH). Electrodes with field potentials of good quality, being the ones with amplitudes of depolarization and repolarization peaks higher than 200 µV and 20 µV, respectively, were selected for further analysis (Ando et al., 2017; Sala et al., 2017; Shi et al., 2020a). Subsequently, two parameters reflecting electrophysiological activity of cardiomyocytes, namely field potential duration (FPD, duration between the beginning of the sodium spike and the repolarizing peak) and RR interval (duration between two depolarization peaks), were measured from the 2 min recording for each concentration.

In line with other MEA studies, the Fridericia formula (Eq. 1) was applied to correct for the effect of beat rate on FPD (Ando et al., 2017; Kitaguchi et al., 2017; Vandenberk et al., 2016):

$$FPDc = \frac{FPD}{\sqrt[3]{RR\ interval}} \quad (1)$$

Where the FPD and RR-interval are expressed in seconds. Well-based FPDc were determined by calculating the relative percentage of FPDc for the exposure measurements compared to FPDc at baseline conditions (0.05% (v/v) acetonitrile or 0.1% (v/v) DMSO) set at 100%. The potential effects of time, addition and vehicle on well-based FPDc were corrected for by subtracting the responses obtained from the corresponding time-matched vehicle control well. Irregular waveforms (Fig. S1[2]) on field potential including arrhythmia-type changes, a flattened unclear second peak and beating arrest may occur at high concentrations (Kitaguchi et al., 2017; Shi et al., 2020a; Zwartsen et al., 2019). For deriving concentration-response curves of model compounds, concentrations inducing irregular waveforms were excluded given the FPD and RR interval could not be defined.

To compare the potency of model compounds, BMD analysis was used to derive effective concentrations causing a defined % increase in the FPDc compared to the baseline control as described in the "Benchmark dose analysis" section. The concentration–response curves were plotted using GraphPad Prism 5.0 with four-parameters logistic fit (GraphPad Software Inc., San Diego, USA). Data were collected from three independent experiments with six well replicates (two replicates for dofetilide and isoproterenol) in each experiment. Each data point is presented as the mean value ± standard deviation (SD) of the three independent replicates. One-way analysis of variance (ANOVA) followed by Dunnett test were conducted to assess the effect of ibogaine and noribogaine on FPDc using GraphPad Prism 5.0 (GraphPad Software Inc.). Significance was determined at $p < 0.05$.

2.4. *In vitro* experimental biokinetic parameters for the PBK models

2.4.1. In vitro intestinal transport studies

To estimate the intestinal absorption of ibogaine and noribogaine, a Caco-2 transport study was performed to determine the apparent permeability coefficients (P_{app}) using a previously developed method with minor modifications (Hubatsch et al., 2007; Strikwold et al., 2017). Caco-2 cells (passages 10-15 post -thawing) were seeded onto the insert of Costar 12-well transwell plates (Corning, 0.4 µm pored polycarbonate membrane, 12 mm diameter). The apical compartment of each well was filled with 0.5 ml of a 4 x 10^4 cell suspension in culture medium consisting of DMEM supplemented with 10% (v/v) FBS, 1% (v/v) P/S and 1% (v/v) NEAA and the basolateral compartment was filled with 1.5 ml culture medium. Given that FBS is an animal-derived components whose production may be associated with pain and suffering, FBS-free culture medium for Caco-2 cells, e.g., serum-free DMEM containing insulin, transferrin, selenium (ITS) or MITO+™ serum extender (ITS plus growth factors) (Ferruzza et al. 2013), could be considered in future Caco-2 transport studies. The plate was incubated under atmospheric conditions at 37℃ and 5% CO_2 for 21-23 days, which allows cells to grow and differentiate into a confluent monolayer. Cell culture medium was changed every 2 days.

Stock solutions of ibogaine were prepared in acetonitrile/water (50/50 v/v). Noribogaine, methadone (reference compound), antipyrine (passive transcellular control for the transport studies) and fluorescein (passive paracellular control for the transport studies) were dissolved in DMSO. Stock solutions were diluted 200-fold resulting a final test concentration of 50 µM (125 nM for fluorescein) at which cytotoxicity was not observed (data not shown). The final concentration of acetonitrile or DMSO was 0.25%(v/v) or 0.5% (v/v), respectively.

For the transport experiment, HBSS containing 10 mM methanesulfonic acid, $NaHCO_3$ (final concentration 0.35 mg/ml) and the respective test compounds was used as exposure medium (pH 6.5) in the apical compartment. HBSS containing 30 mg/ml BSA was used as medium in the basolateral compartment (pH 7.4). 1.5 ml basolateral transport medium was first added, and the experiment was initiated by adding 0.5 ml exposure medium to the apical compartment. The plate was incubated at 37 °C with 5% CO_2 for 20 min. Subsequently, an aliquot of 75 µl sample was collected from the basolateral compartment and transferred to a tube containing 150 µl ice-cold acetonitrile. To measure the mass balance (recovery), 75 µl exposure buffer was also collected from the apical compartment before and after the incubation and added to the tubes containing 150 µl ice-cold acetonitrile. The insert filters were washed with PBS then cut out and transferred to 200 µl ice-cold acetonitrile for a 15 min sonification. Samples were left on ice for 20 min and centrifuged for 45 min at 18,000g, after which supernatants were collected for LC-MS/MS analysis.

To check the linearity of transport of test compounds, 75 µl sample was collected from the basolateral compartment at 1, 5, 10, 20, 30 and 60 min of incubation and added to 150 µl ice-cold acetonitrile. After each collection, an equal volume of basolateral transport medium was added back as compensation. The calculation for each time point was corrected for the dilutions.

The integrity of the Caco-2 cell monolayer was checked by measuring the transepithelial electrical resistance (TEER) using a Millicell ERS-2 Volt–Ohm Meter (EMD Millipore Corporation, California, USA). Prior to the transport experiment, cells

[2] doi:10.14573/altex.2103311s

with a TEER value between 600 and 800 Ωcm^2 were chosen for the transport study. After the experiment, cells with a change of TEER value larger than 20% were excluded from further analysis of the P_{app} value (Bentz et al., 2013). Additionally, the integrity was also checked by measuring the transport of fluorescein, and cells with a transport of fluorescein less than 1 % were considered suitable for the analysis.

The P_{app} (cm/s) value was calculated using Eq. 2 as follows (Hubatsch et al., 2007; Strikwold et al., 2017):

$$P_{app} = \frac{\Delta Q/\Delta t}{A \times C_0} \quad (2)$$

where $\Delta Q/\Delta t$ (nmol/s) is the amount of the test compound transported to the basolateral compartment over the incubation time, A (cm^2) is the surface area of the filter and C_0 (µM) is the initial concentration of the test compound in the apical compartment. The mass balance was calculated by comparing the total amount of compound in the apical compartment, basolateral compartment, and filter to the initial amount. The results were obtained from three independent experiments including four replicates for ibogaine and noribogaine and two replicates for methadone and antipyrine in each independent experiment. Data are presented as the mean value ± SD.

Using methadone as a reference compound, the *in vivo* oral absorption rate constant (ka) for ibogaine and noribogaine were calculated by multiplying the corresponding ratio of P_{app} to P_{app} of methadone by a mean ka value of methadone being 0.59/h reported in human studies (Foster et al., 2000; Wolff et al., 2000).

2.4.2. In vitro microsomal incubations

To determine kinetic parameters for the conversion of ibogaine to noribogaine, *in vitro* microsomal incubations were performed as described before (Shi et al., 2020a) with minor modifications. Incubation mixtures contained the NADPH regeneration system (final concentrations 1.3 mM $NADP^+$, 3.3 mM glucose-6-phosphate, 0.4 U/ml glucose-6-phosphate dehydrogenase and 3.3 mM $MgCl_2$) and ibogaine at final concentrations from 0 to 25 µM, in 100 mM Tris-HCl buffer (pH 7.4) with a total volume of 160 µl. Stock solutions of ibogaine were prepared in acetonitrile/water (50/50 v/v), and were diluted 50 times to reach the test concentrations in the incubation mixtures. Samples were pre-incubated at 37°C for 1 min and a final concentration of 0.25 mg/ml liver microsomal protein was added to initiate the reaction. After 2.5 min incubation in a shaking water bath at 37 °C, the reaction was terminated by adding 40 µl ice-cold acetonitrile. Control incubations were performed in the absence of NADPH which was replaced with Tris-HCl.

The formation of the glucuronide of noribogaine was investigated in a similar manner as described above. A total volume of 200 µl sample contained (final concentrations) UGT reaction system (5 mM uridine 5′-diphosphoglucuronic acid (UDPGA), 8 mM $MgCl_2$, 25 µg/ml alamethicin) and 0.5 mg/ml liver microsomal protein in 100 mM Tris–HCl (pH 7.4). Samples were placed on ice for 30 min which allows the pore forming peptide alamethicin to boost the glucuronidation activity (Fisher et al., 2000; Ning et al., 2017). After pre-incubating samples at 37°C for 5 min, reactions were started by adding noribogaine from 100 times concentrated stock solutions in DMSO at final concentrations ranging from 0-750 µM. The incubation time was 40 min and reactions were terminated by adding 50 µl ice-cold acetonitrile. Control incubations were performed in the absence of UDPGA which was replaced with Tris-HCl.

Test concentrations of ibogaine and noribogaine were chosen at relevant human plasma concentrations and enabled the determination of Michaelis-Menten kinetic parameters. Optimizations of experiments demonstrated that the reaction rates for the formation of noribogaine were linear with time up to 20 min and with protein concentration of up to 1 mg/ml. For the formation of noribogaine glucuronides, reaction rates were shown to be linear with time up to 120 min and with protein concentration up to 0.75 mg/ml. After termination, samples were centrifuged at 18,000 g for 5 min at 4 °C. The supernatant was collected for the quantification of ibogaine, noribogaine and noribogaine glucuronide by liquid chromatography-mass spectrometry (LC-MS/MS) as described in the "LC-MS/MS analysis" section.

For the kinetic analysis, the data for the formation of noribogaine and noribogaine glucuronide were fitted to the Michaelis-Menten Eq. 3 using GraphPad Prism 5.0 (GraphPad Software Inc.):

$$v = \frac{V_{max} \times [S]}{K_m + [S]} \quad (3)$$

where [S] is the substrate concentration (µM) and v is the rate of metabolite formation (nmol/min/mg protein). V_{max} is the apparent maximum velocity (nmol/min/mg protein) and K_m the apparent Michaelis–Menten constant (µM). The *in vitro* catalytic efficiency expressed in µl/min/mg microsomal protein was calculated by dividing V_{max} by K_m. Data were collected from three independent experiments and each data point is presented as the mean value ± SD.

2.5. Determination of plasma protein and *in vitro* medium binding

The rapid equilibrium dialysis (RED) assay was conducted to determine the unbound fraction (f_u) of ibogaine and noribogaine in pooled human plasma and in the *in vitro* medium used in the hiPSC-CM MEA assay as previously described (Shi et al., 2020a). The stock solutions of ibogaine prepared in acetonitrile/water (50/50 v/v) and noribogaine dissolved in DMSO were diluted 100-fold in human plasma or *in vitro* medium to reach the final concentration of 10 µM in test sample solutions. A 300 µl aliquot of test sample solution was added to the sample chamber and 500 µl PBS was added to the buffer chamber of the RED insert, after which dialysis was performed on an orbital shaker at 37 °C at 250 rpm for 5 h. Following dialysis, an aliquot of 25 µl was collected from both the sample and buffer chamber and diluted with 25 µl of PBS (to the aliquot from the sample chamber) and plasma or *in vitro* medium (to the aliquot from the buffer chamber) to eliminate potential matrix effects. Subsequently, post-treatment samples were precipitated using 300 µl cold acetonitrile/water (50/50 v/v) and left on ice for 30 min followed by a centrifugation for 45 min

at 18,000g. Supernatants were collected for LC-MS/MS analysis. The fraction unbound (f_u) was calculated with Eq. 4 (van Liempd et al., 2011; Waters et al., 2008):

$$f_u = \frac{\text{concentration in buffer chamber}}{\text{concentration in sample chamber}} \quad (4)$$

The measurements were performed in triplicate in three independent experiments. Results are presented as the mean value ± SD.

2.6. LC-MS/MS analysis

The identification and quantification of compounds in samples from the Caco-2 transport studies, microsomal incubation and RED assay were performed by LC-MS/MS analysis using a Shimadzu Nexera XR LC-40D SR UPLC system coupled with a Shimadzu LCMS-8045 mass spectrometer (Kyoto, Japan). The compounds were separated by a Phenomenex Kinetex® C18 column (2.1 x 50 mm 1.7 µm, 100 Å) connected to a precolumn and detected by a Shimadzu LCMS-8045 triple quadrupole with electrospray ionization (ESI) interface. The instrument was operated in positive mode and multiple reaction monitoring (MRM, N_2 collision gas) mode. The MRMs of m/z 311.15 (MH^+) to 122.2 (CE: – 33 kV), m/z 311.15 (MH^+) to 174.2 (CE: – 36 kV) and m/z 311.15 (MH^+) to 124.15 (CE: – 31 kV) were used to analyze ibogaine. The MRMs of m/z 297 (MH^+) to 122.15 (CE: – 33 kV), m/z 297 (MH^+) to 160.2 (CE: – 35 kV) and m/z 297 (MH^+) to 146.25 (CE: – 45 kV) were used to analyze ibogaine. The MRMs of m/z 473.15 (MH^+) to 297.2 (CE: – 33 kV), m/z 473.15 (MH^+) to 122.15 (CE: – 54 kV) and m/z 473.15 (MH^+) to 160.1 (CE: – 50 kV) were used to analyze noribogaine glucuronide. The MRMs for methadone were m/z 310.2 (MH^+) to 265.15 (CE: – 15 kV), m/z 310.2 (MH^+) to 105.05 (CE: – 29 kV) and m/z 310.2 (MH^+) to 77.15 (CE: – 50 kV). The MRMs for antipyrine were m/z 189.1 (MH^+) to 56.1 (CE: – 35 kV), m/z 189.1 (MH^+) to 77.2 (CE: – 42 kV) and m/z 189.1 (MH^+) to 58.2 (CE: – 23 kV). The MRMs were selected based on previous studies (Chang et al., 2011; Glue et al., 2016).

Mobile phase A was nanopure water containing 0.1% (v/v) formic acid and mobile phase B was acetonitrile containing 0.1% (v/v) formic acid. A gradient elution at a flow rate of 0.3 ml/min was applied for the analysis with the program set as follows: the initial concentration was 100% mobile phase A, linearly changing to 100% mobile phase B over 7 min which was held for 1 min. Then mobile phase B dropped to 0% over 1 min followed by equilibration of the system for 4 minutes. Total run time was 13 minutes. The injection volume was 1 µl and the temperature of the column was kept at 40 °C. The retention times for ibogaine, noribogaine, noribogaine glucuronide, methadone and antipyrine were 5.6, 5.0, 4.9, 6.3 and 5.1 min, respectively, determined using commercially available reference compounds. Quantification was performed by comparing the respective peak areas of the total ion chromatogram (TIC) to the TIC peak areas of corresponding linear calibration curves of reference compounds ($R^2 > 0.999$), using Browser analysis in the software LabSolution (Shimadzu).

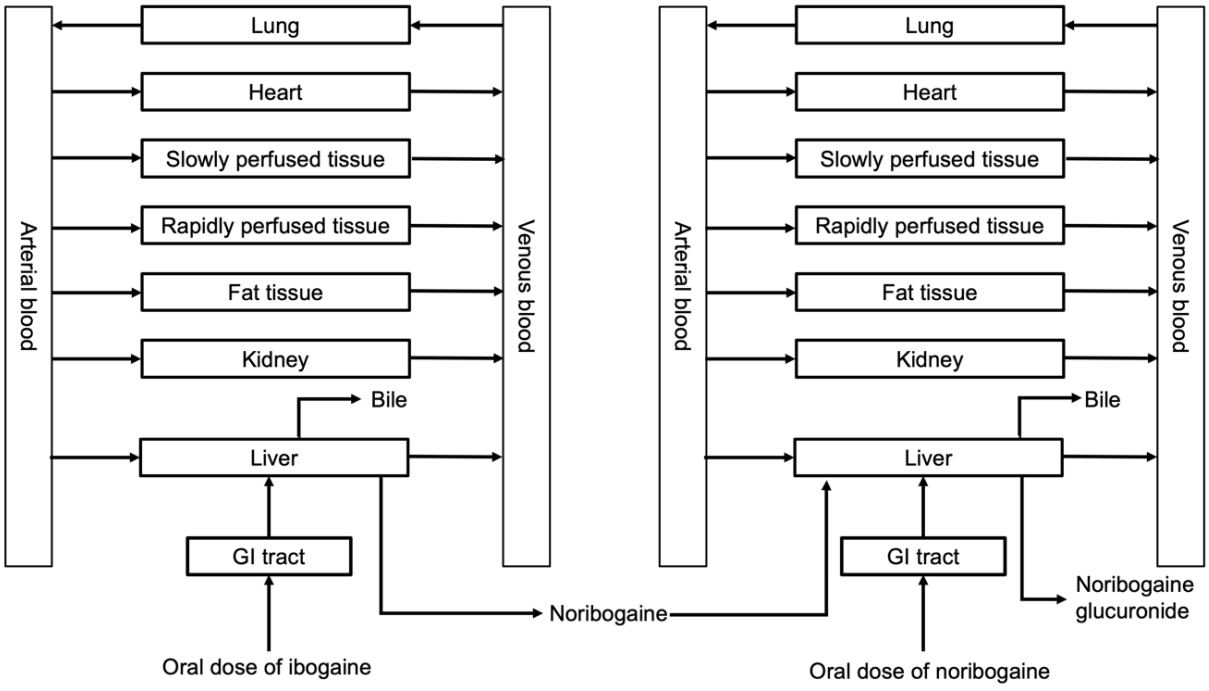

Fig. 4: Schematic diagram of the PBK model for ibogaine with a submodel for noribogaine

2.7. PBK models development and evaluation

A PBK model consisting of multiple organ compartments was developed to describe the ADME of ibogaine and its metabolite noribogaine upon oral administration (Figure 4). Noribogaine has also been reported to cause the prolongation effects on the QTc interval in human (Glue et al., 2016). Therefore, an oral administration route was included in the submodel of noribogaine (Figure 4), which enables modeling of noribogaine kinetics and prediction of its cardiotoxicity upon oral administration. A full description of the model development can be found in the Text S1 and Tables S2 and S3[2]. Kinetic model calculations were performed with Berkeley Madonna (version 8.3.18, UC Berkeley, CA, USA), applying Rosenbrock's algorithms for solving stiff systems. Model equations are shown in Text S2[2].

To evaluate the model, the predicted blood concentrations and area under the blood concentration- time curve (AUC) of ibogaine and noribogaine were compared with the *in vivo* data reported in clinical studies (Glue et al., 2015a,b 2016). The reported plasma-based kinetics of ibogaine and noribogaine were extracted using WebPlotDigitizer Version 4.4. (Rohatgi, 2020) and converted to blood-based kinetics by multiplying with the respective blood to plasma ratio (BPr) values. The evaluation was performed according to the specifications (body weight and oral dose) of *in vivo* studies as summarized in Table 2. A local parameter sensitivity analysis was conducted to estimate to what extent the model parameters can influence the model output. A full description of the sensitivity analysis and results can be found in the Text S3 and Figure S5[2].

2.8. QIVIVE using PBK modeling-based reverse dosimetry

Given that the *in vitro* endpoint FPDc can be considered as a surrogate endpoint for the QTc interval in the human ECG (Shi et al., 2020a; Zwartsen et al., 2019), *in vitro* concentration-response curves for FPDc obtained in the hiPSC-CM MEA assay were translated to *in vivo* dose-response curves for QTc using PBK modeling-based reverse dosimetry. In the case of oral administration of ibogaine, a toxic equivalence (TEQ) approach was applied to combine the cardiotoxicity of ibogaine and noribogaine. Assuming that the cardiotoxicity of ibogaine and noribogaine are additive to hiPSC-CM, the internal unbound TEQ concentration was the combination of the unbound concentration of ibogaine and noribogaine in the heart venous blood taking the corresponding toxic equivalency factors (TEFs) into account. The TEF of ibogaine and noribogaine were calculated based on their cardiotoxic potencies obtained in the hiPSC-CM MEA assay, with the TEF for ibogaine defined as 1.00. Then QIVIVE was performed by assuming the *in vitro* unbound concentration of ibogaine equal to the unbound C_{max} of unbound ibogaine expressed in TEQ concentrations in the heart venous blood as shown in the Eq.5 and 6:

$$C_{total,\ in\ vitro,\ ibo} \times f_{u,\ m,\ ibo} = C_{unbound,\ human\ blood,\ TEQ} \quad (5)$$

$$C_{unbound,\ human\ blood,\ TEQ} = C_{total,\ human\ blood,\ ibo} \times \frac{f_{u,\ p,\ ibo}}{BPr_{\ ibo}} \times TEF_{\ ibo} + C_{total,\ human\ blood,nor} \times \frac{f_{u,\ p,nor}}{BPr_{\ nor}} \times TEF_{nor} \quad (6)$$

where $C_{total,\ in\ vitro,ibo}$ and $f_{u,\ m,\ ibo}$ are the *in vitro* ibogaine concentration and unbound fraction of ibogaine in the *in vitro* exposure medium, respectively. BPr_{ibo} and BPr_{nor} are the blood to plasma ratio of ibogaine and noribogaine. $f_{u,\ p,\ ibo}$ and $f_{u,\ p,\ nor}$ are the respective unbound fraction of ibogaine and noribogaine in human plasma. $C_{total,\ human\ blood,\ ibo}$ and $C_{total,\ human\ blood,\ nor}$ are the concentrations of ibogaine and noribogaine in the heart venous blood, respectively. TEF_{ibo} and TEF_{nor} are the TEF values of ibogaine (defined as 1.00) and noribogaine (defined based on its relative potency in the MEA assay). $C_{unbound,\ human\ blood,\ TEQ}$ values were converted to *in vivo* oral doses of ibogaine by PBK-modeling based reverse dosimetry, using a bodyweight of 70 kg (Brown et al., 1997).

When oral administration of noribogaine was considered, the translation was performed by setting the *in vitro* unbound concentrations of noribogaine detected in the hiPSC-CM MEA assay equal to the unbound C_{max} of noribogaine in the heart venous blood with a correction for the fraction unbound in human plasma and conversion from plasma to blood using BPr as described in in Eq.7:

$$C_{total,\ human\ blood,\ nor} = \frac{C_{total,\ in\ vitro,\ nor} \times f_{u,\ m,\ nor}}{\frac{f_{u,\ p,\ nor}}{BPr_{\ nor}}} \quad (7)$$

where $C_{total,\ in\ vitro,nor}$ and $f_{u,\ m,\ nor}$ are the *in vitro* noribogaine concentration and unbound fraction of noribogaine in the *in vitro* exposure medium, respectively. $C_{total,\ human\ blood,\ nor}$ values were extrapolated to *in vivo* oral doses of noribogaine by PBK-modeling based reverse dosimetry, using a bodyweight of 70 kg (Brown et al., 1997). The calculations by Eq. 5 and 6 or 7 were performed for each of the *in vitro* concentrations of ibogaine or noribogaine tested in the hiPSC-CM MEA assay, which enables the translation of the entire *in vitro* concentration-response curve to a predicted *in vivo* dose-response curve.

2.9. Validation of the PBK modeling-based reverse dosimetry approach

To validate the performance of the PBK modeling-based reverse dosimetry approach, the predicted dose-response curves for QTc prolongation upon the exposure to ibogaine and noribogaine were compared to the respective *in vivo* dose-response data obtained from single case reports and clinical studies (Asua, 2013; Glue et al., 2016; Grogan et al., 2019; Henstra et al., 2017; Hildyard et al., 2016; Hoelen et al., 2009; Meisner et al., 2016; Pleskovic et al., 2012; Steinberg and Deyell, 2018; Vlaanderen et al., 2014). Since in most case reports ibogaine administered to the patients were internet-purchased with unknown purity, the reported doses were converted to effective doses by multiplying with the lower (15%) and upper value (50%) of purity reported in Alper et al. (2012). The predicted dose-response curve of noribogaine for the validation was made using the bodyweight of 81.9 kg, which was the average body weight of subjects as reported in Glue et al. (2016). The details of the *in vivo* studies are summarized in Table S1[2] in the supplementary material. The *in vitro* absolute FPDc values and the *in vivo* QTc data were expressed as relative percentages by comparing the post-treatment data to the baseline values for a straightforward comparison.

ALTEX, accepted manuscript
published July 16, 2021
doi:10.14573/altex.2103311

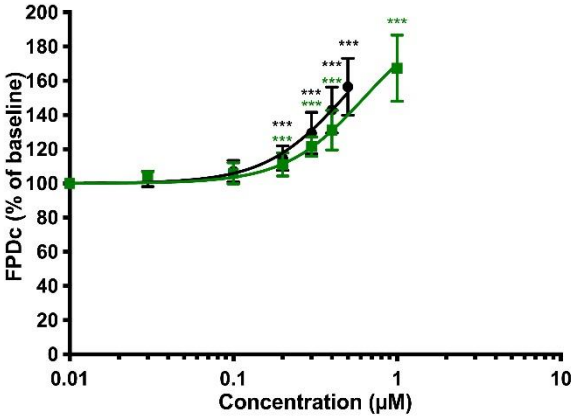

Fig. 5: Concentration-response curves for the effect of ibogaine (black circles and line) and noribogaine (green squares and line) on FPDc in hiPSC-CM detected by the MEA
The response of the baseline condition (0.05% (v/v) acetonitrile for ibogaine, 0.1% (v/v) DMSO for noribogaine) was set at 100%. Data represent the mean of results obtained from three independent experiments each containing six well replicates. Each data point represents the mean ± SD. Statistically significant changes in response compared to the solvent control are marked with * with $p < 0.001$: ***.

2.10. Benchmark dose analysis

BMD analysis of reported and predicted dose-response curves for ibogaine and noribogaine was performed to derive a lower 95% confidence limit of the BMD resulting in 10% cardiotoxicity ($BMDL_{10}$), which can be used as the point of departure (PoDs) for the risk assessment and safety evaluation of ibogaine and noribogaine. As previously described (Shi et al., 2020a), an effective size of 10% was chosen based on the fact that a $BMDL_{10}$ value is generally considered as a dose level similar to a no observed adverse effect level (EFSA, 2017), and that 10% change in QTc interval over the population baseline of 407 ms, being a QTc of 450 ms can be used as a threshold to evaluate the abnormal QTc prolongation (ICH 2005; Mujtaba et al. 2013; Wedam et al. 2007; Florian et al. 2012). The European Food Safety Authority web-tool based on R-package PROAST version 69 (Dutch National Institute for Public Health and the Environment, RIVM, The Netherlands) was used for the BMD analysis (Shi et al., 2020a).

BMD analysis of *in vitro* concentration-response data was performed to calculate the benchmark concentrations (BMC) resulting in 10% change in the FPDc with lower 95% confidence limit ($BMCL_{10}$). The obtained $BMCL_{10}$ values were used to compare the potency and derive the TEF of noribogaine relative to the TEF of ibogaine set at 1.00.

3 Results

3.1. *In vitro* cardiotoxicity of ibogaine and noribogaine in the hiPSC-CM MEA assay

Figure 5 shows that ibogaine and its metabolite noribogaine induced a significant concentration-dependent prolongation of FPDc. The $BMCL_{10}$ is 0.11 µM for ibogaine and 0.15 µM for noribogaine, which results in TEF values of ibogaine and noribogaine being 1.00 and 0.65, respectively. Arrhythmia-type waveforms were observed upon the treatment with 1 µM ibogaine and 3 µM noribogaine. The repeated addition of vehicle controls (0.05% (v/v) acetonitrile and 0.1% (v/v) DMSO) did not significantly influence the FPDc (Fig. S2[2]). Two reference compounds dofetilide and isoproterenol respectively prolonged the FPD_C and increased beat rates in a concentration-dependent manner, indicating the adequate performance of the hiPSC-CM MEA assay (Fig. S3[2]).

3.2. *In vitro* experimental biokinetic parameters for PBK models

3.2.1. In vitro intestinal transport studies

Table 1 shows the P_{app} values obtained from Caco-2 transport studies and the ka values of the test compounds derived from these P_{app} values based on comparison to the data for methadone. All test compounds were rapidly transported with the largest P_{app} value of 47.0 $x10^{-6}$ cm/s for antipyrine and the smallest P_{app} value of 20.8 $x10^{-6}$ cm/s for methadone. The P_{app} value of noribogaine was 1.5-fold higher than that of ibogaine. The transport of all test compounds was within the linear range up to 30 min of incubation. The mass recovery of ibogaine, noribogaine, methadone and antipyrine are 90%, 102%, 74% and 88%, respectively.

3.2.2. In vitro microsomal incubations

Figure S4[2] shows the substrate concentration dependent metabolism of ibogaine and noribogaine by human liver microsomes. The obtained results follow Michaelis-Menten kinetics. The apparent V_{max} and K_m derived from these data for the formation of noribogaine from ibogaine were 0.17 ± 0.033 nmol/min/mg microsomal protein and 0.63 ± 0.005 µM, respectively. The apparent V_{max} and K_m for the conversion of noribogaine to its glucuronide were 0.036 ± 0.0008 nmol/min/mg microsomal protein and 305 ± 15.8 µM, respectively. The catalytic efficiency (V_{max}/K_m) for the formation of noribogaine was 269.8 µl/min/mg microsomal protein, which was 2,248-fold more efficient than that for formation of noribogaine glucuronide being 0.12 µl/min/mg microsomal protein. This explains the relatively higher plasma concentrations of noribogaine than of ibogaine upon dosing ibogaine (see below).

Tab. 1: The apparent permeability (P_{app}) obtained from Caco-2 transport studies, and the predicted intestinal oral absorption rate constants (ka) for the test compounds derived from the P_{app} values using the ka for methadone (Foster et al., 2000; Wolff et al., 2000) as the reference

Compound	P_{app} ± SD (10^{-6} cm/s)	ka (/h)
Ibogaine	27.9 ± 4.6	0.79
Noribogaine	42.4 ± 3.6	1.23
Methadone	20.8 ± 1.9	0.59 [a]
Antipyrine	47.0 ± 5.0	1.33

[a] Reported value obtained from human studies (Foster et al., 2000; Wolff et al., 2000)

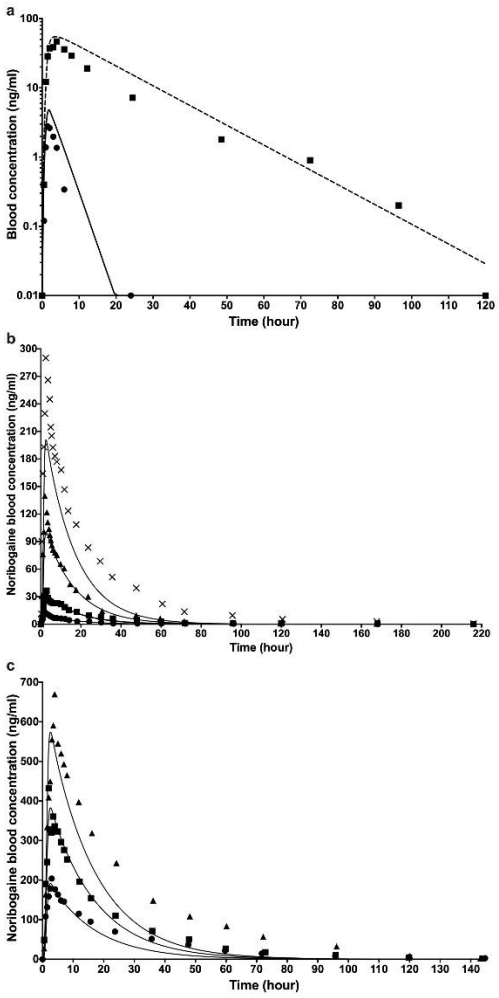

Fig. 6: Comparison of blood concentration-time curves of ibogaine and noribogaine in human predicted with the PBK model and as published in the literature for human case studies
(a) Dots and squares respectively indicate the reported blood concentrations of ibogaine and noribogaine after a single oral dose of 20 mg ibogaine (Glue et al., 2015b). Solid lines and dashed lines represent the predictions for ibogaine and noribogaine, respectively. **(b)** Dots, squares, triangles and crosses represent the reported blood concentrations after an oral dose of 3, 10, 30 and 60 mg noribogaine (Glue et al., 2015a), respectively, with the solid lines being the predicted blood concentrations for the corresponding doses. **(c)** Dots, squares, and triangles represent the reported blood concentrations after an oral dose of 60, 120 and 180 noribogaine (Glue et al., 2016), respectively, with the solid lines being the predicted blood concentrations of the corresponding doses.

3.3. Determination of plasma protein and *in vitro* medium binding

The unbound fraction of ibogaine and noribogaine in the *in vitro* medium and human plasma were determined by the RED assay, in order to enable the calculation of the unbound concentration of the compounds for the *in vitro* to *in vivo* extrapolation. The unbound fraction of ibogaine and noribogaine in the *in vitro* medium were comparable, amounting to 0.71 ± 0.01 and 0.80 ± 0.03, respectively. The unbound fraction of ibogaine in human plasma was determined to be 0.04 ± 0.017, which was 6.5-fold lower than that for noribogaine, being 0.26 ± 0.05.

3.4. Evaluation of the PBK model

The PBK models of ibogaine and noribogaine were evaluated against *in vivo* data reported in clinical studies. Figure 6 shows that the developed PBK model accurately predicted the time-dependent change in the blood concentrations of ibogaine and noribogaine upon oral administration of ibogaine (Glue et al., 2015b) and noribogaine (Glue et al., 2015a, 2016) with differences between the

predicted and reported blood C_{max} and AUC being less than around 2-fold, which is generally considered as an adequate predictive performance (Badhan et al. 2019; WHO 2010). The detailed comparisons between predicted and reported blood C_{max} and AUC values are summarized in Table 2. For ibogaine, the predicted blood C_{max} and AUC were 1.7- fold and 2.1-fold higher than the reported values, respectively. For noribogaine, the prediction shows an average 0.9-fold and 1.3-fold difference both in blood C_{max} and AUC values.

3.5 Contribution of ibogaine and noribogaine to blood ibogaine equivalents

To further illustrate the contribution of ibogaine and noribogaine to ibogaine-induced cardiotoxicity in human, a dose-dependent comparison was made between the predicted unbound blood concentration of ibogaine and noribogaine considering their TEF values. Figure 7 shows that, upon dosing ibogaine, the contribution of noribogaine to the C_{max} expressed in unbound ibogaine equivalents is substantially higher than the contribution of ibogaine itself at all dose levels evaluated. The relative contribution of ibogaine to the ibogaine equivalents increases with increasing oral dose but is still about 8-fold lower than that of noribogaine at 500 mg, in spite of the only limited difference in the TEF value between the two compounds. This observation can be ascribed to the fact that the concentration of noribogaine is higher than that of ibogaine (see also Figure 6a) due to the fact the catalytic efficiency of ibogaine O-demethylation to noribogaine is more efficient than the clearance of noribogaine by glucuronidation.

3.6 QIVIVE using PBK modeling-based reverse dosimetry, its validation and BMD analysis

By applying reverse dosimetry, the *in vitro* concentration-response curves of ibogaine and noribogaine obtained in the hiPSC-CM MEA assay were translated to predicted *in vivo* dose-response curves for the QTc prolongation, upon oral administration of ibogaine (Figure 8a) or noribogaine (Figure 8b). Subsequently, the predicted data were compared to the *in vivo* dose-response data for QTc

Tab. 2: Summary of *in vivo* kinetic studies and evaluation of the PBK model predictions for ibogaine and noribogaine blood C_{max} and AUC

Compound	Mean body weight (kg)	Mean dose (mg/day)	*In vivo* C_{max} (ng/ml) [a]	Predicted C_{max} (ng/ml)	Ratio predicted C_{max}/*in vivo* C_{max}	In *vivo* AUC (ng*h/ml) [a]	Predicted AUC (ng*h/ml)	Ratio predicted AUC/in *vivo* AUC	Reference
Ibogaine	80 [b]	20	2.75	4.80	1.7	9.0	19.2	2.1	Glue et al. (2015b)
Noribogaine		- [d]	46.8	54.8	1.2	693.5	1027.1	1.5	
Noribogaine	78	3	13.0	10.0	0.77	185.5	165.8	0.89	Glue et al. (2015a)
		10	36.3	33.5	0.92	636.25	552.8	0.87	
		30	139.8	100.4	0.72	1751.0	1658.4	0.95	
		60	290.0	200.8	0.69	4905.5	3316.9	0.68	
Noribogaine	81.9	60	204.0	191.3	0.94	5150.8	3924.1	0.76	Glue et al. (2016)
		120	432.0	382.7	0.89	8201.3	7848.5	0.96	
		180	669.8	574.1	0.86	17219.3	11773.3	0.68	

[a] Blood data were obtained by multiplying reported plasma data by the BPr value.
[b] The body weight was not reported and set equal to the average of values in other studies conducted by the same group (Glue et al., 2016; Glue et al., 2015a), assuming subjects have similar demographic characteristics.
[c] The body weight was not reported and set equal to the value used in the PBK model.
[d] Subjects were administered ibogaine.

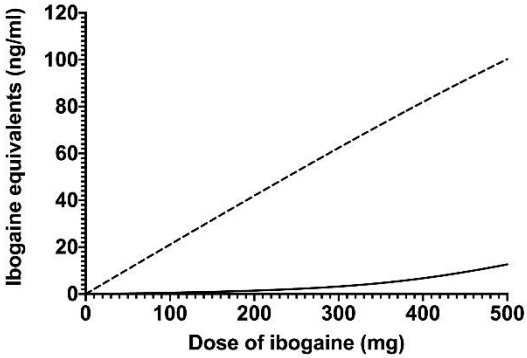

Fig. 7: Predicted dose-dependent relative contribution of ibogaine (solid line) and noribogaine (dashed line) to the C_{max} expressed in unbound ibogaine equivalents for a human of 70 kg

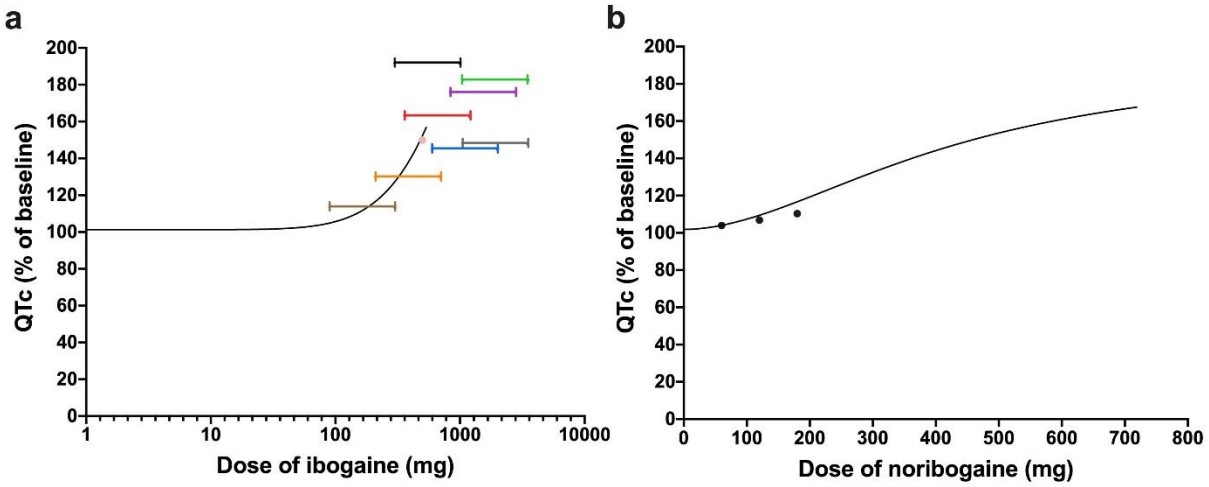

Fig. 8: Predicted dose–response curves for cardiotoxicity of (a) ibogaine and (b) noribogaine obtained using PBK modeling-based reverse dosimetry compared to *in vivo* data derived from literature
The curves represent the predicted dose dependent QTc prolongation. Horizontal bars or the dot in **(a)** represent the reported data of ibogaine obtained from the following studies: Asua (2013) (grey); Grogan et al. (2019) (black); Henstra et al. (2017) (orange); Hildyard et al. (2016) (green); Hoelen et al. (2009) (pink dot); Meisner et al. (2016) (blue); Pleskovic et al. (2012) (brown); Steinberg and Deyell (2018) (purple); Vlaanderen et al. (2014) (red). The horizontal bars represent the range of effective doses corrected by multiplying the reported doses with the purity range of internet-purchased ibogaine (15-50%) (Alper et al. 2012). Dots in **(b)** represent the *in vivo* dose-response data for noribogaine reported in Glue et al. (2016).

prolongation obtained from case studies and clinical studies to evaluate the performance of the PBK modeling-based reverse dosimetry predictions (Figure 8). Given the unknown purity of internet-purchased ibogaine described in the case studies, a range of 15 to 50% was used to correct for the effective doses. Figure 8a reveals that the predicted dose-dependent QTc prolongation for ibogaine is best in line with the reported data when the a purify of 15% was considered. For noribogaine, the predicted dose-response curve is comparable with the reported dose-response data on QTc prolongation (Figure 8b).

To further evaluate the model predictions and derive PoDs for risk assessment, $BMDL_{10}$ values were calculated from both predicted and reported dose-response curves. The $BMDL_{10}$ value of noribogaine derived from the clinical study of Glue et al. (2016) was 163 mg for the subjects with an average body weight of 81.9 kg, which is 1.5-fold higher than the predicted $BMDL_{10}$ value amounting to 110 mg for a 81.9 kg person, showing that the PBK modeling-based reverse dosimetry can adequately predicted the *in vivo* cardiotoxicity of noribogaine. The predicted $BMDL_{10}$ value for ibogaine-induced QTc prolongation was 108 mg for a 70 kg person, which is similar to that for noribogaine (94.2 mg, based on a bodyweight of 70 mg), indicating a comparable potency of the two compounds in inducing QTc prolongation.

4 Discussion and conclusion

The aim of the present study was to provide an additional proof-of-principle for the potential prediction of *in vivo* human cardiotoxicity on QTc prolongation by combing an *in vitro* cardiotoxicity assay, *in vitro*-derived biokinetic parameters and PBK modeling-based reverse dosimetry as a NAM for human risk and safety assessment. Two herbal alkaloids, ibogaine and noribogaine being promising anti-addiction drugs, were selected as model compounds since their cardiotoxicity is one of the major safety concerns related to their clinical uses, while so far not well studied. In addition, available *in vivo* kinetic and QTc data available for human subjects exposed to the compounds enable the evaluation of the developed NAM against clinically observed responses.

In the current paper, the electrophysiological cardiotoxicity of ibogaine and noribogaine was assessed using hiPSC-CMs on the MEA platform, which has been used previously for detecting drug-induced QTc prolongation and proarrhythmia (Shi et al., 2020a,b; Satsuka and Kanda, 2020). The results reveal that ibogaine and noribogaine prolonged the FPDc in a concentration-dependent manner which could be explained by their inhibitory effects on hERG channels as detected using human mammalian cell lines heterologously expressing hERG channels (Alper et al., 2016; Koenig et al., 2014; Rubi et al., 2017). Our results also indicate that ibogaine was 1.4-fold more potent than noribogaine in prolonging FPDc, which is in contrast to those hERG inhibition studies reporting a slightly lower (1.3-fold) potency of ibogaine compared to noribogaine. The discrepancy might be ascribed to the usage of different cell models. Unlike transfected cell lines containing a single type of ion channels, hiPSC-CMs express the major cardiac ion channels and receptors present in human cardiomyocytes (Karakikes et al., 2015; Kussauer et al., 2019; Ma et al., 2011) and thus the observed results of ibogaine and noribogaine could be the result of multiple ion-channel effects. Rubi et al. (2017) assessed the cardiotoxicity of ibogaine and noribogaine in hiPSC-CMs using one concentration of each compound which

prolonged the action potential duration at 90% repolarization by respectively 14.2% and 15.5% indicating comparable potency. Additionally, arrhythmia-type waveforms were observed upon treatment of hiPSC-CMs with ibogaine at high concentrations which is line with case studies where cardiac arrhythmia has been associated with the intake of an overdose ibogaine (Asua, 2013; Paling et al., 2012).

Furthermore, at clinically relevant doses of ibogaine for the treatment of drug addiction (typically 500-1000 mg), the total blood concentration of noribogaine ranged from 0.7 to 4.5 µM (Mash et al., 2018) and unbound blood concentrations ranged from 0.08 to 0.47 µM when taking its unbound fraction in plasma and BPr into account. These values cover the unbound *in vitro* effective concentration ($BMCL_{10}$) of noribogaine being 0.12 µM, a value corrected for the unbound fraction in the *in vitro* medium obtained in the current study, indicating that the cardiotoxicity of noribogaine contributes to ibogaine-induced cardiotoxicity and should thus be considered in the reverse dosimetry.

Results obtained from *in vitro* microsomal incubations reveal a high catalytic efficiency for the metabolism of ibogaine to noribogaine, which is in accordance with published data indicating that ibogaine is a compound with high intrinsic clearance with the majority being metabolized to noribogaine (Obach et al., 1998). Based on studies with human liver microsomes Obach et al. (1998) suggested that two enzymes with different activities were involved in the formation of noribogaine, and the apparent V_{max} and K_m for the high-affinity enzyme appeared comparable with our data. However, the reported biphasic kinetics were not observed in our incubations. Furthermore, we found that the catalytic efficiency for the conversion of noribogaine to noribogaine glucuronide was quite low, which is consistent with the fact that only small amounts of noribogaine glucuronides were reported to be formed following an oral dose of noribogaine (Glue et al., 2015a). The substantially higher catalytic efficiency for conversion of ibogaine to noribogaine than for glucuronidation of noribogaine is also reflected by the kinetic data of the present study, and explains why upon dosing ibogaine, plasma levels of noribogaine exceed those of ibogaine itself. Additionally, by comparing the unbound blood concentration corrected for TEF values of ibogaine and noribogaine, we found that noribogaine is predicted to be a major contributor to the unbound TEQ concentration expressed in ibogaine equivalents. In the light of these findings, it can be speculated that noribogaine instead of ibogaine itself plays a dominant role in the *in vivo* cardiotoxicity upon the oral administration of ibogaine. The discrepancy between the relatively high cardiotoxic potency for ibogaine observed in hiPSC-CM MEA assay and a relatively small contribution to the *in vivo* cardiotoxicity could be explained by our findings that i) ibogaine can be efficiently and extensively metabolized to noribogaine, ii) that ibogaine highly binds to the plasma protein, resulting a small unbound internal concentration of ibogaine, which is the fraction generally assumed to be responsible for the therapeutic or toxic effect of drugs (Smith et al., 2010), and iii) that clearance of noribogaine to its glucuronide is less efficient and iv) that the protein binding of noribogaine is somewhat less than that of ibogaine resulting in higher unbound concentrations.

The blood C_{max} and AUC values of ibogaine and noribogaine predicted by the developed PBK model are comparable with the literature data with differences between the predicted and reported values being less than 2-fold, indicating an adequate predictive performance of the developed PBK models.

Based on the sensitivity analysis (Text $S3^2$), the influence of metabolic parameters on the predicted C_{max} of ibogaine in heart venous blood showed a dose-dependent change. When the oral dose of ibogaine increased to 500 mg the influence of V_{max} increased while K_m was less influential. This may be explained by the fact that at high dose levels metabolism gets saturated, which reduces the influence of the K_m with metabolic clearance being dependent on V_{max}. It is also of interest to note that most of the ibogaine related parameters, including metabolic parameters, were not influential to the unbound TEQ concentration expressed in ibogaine equivalents, which however was sensitive to noribogaine related parameters. Furthermore, results show that the unbound TEQ concentration and C_{max} of noribogaine in the heart venous blood were affected by these noribogaine related parameters to a similar extent.

Upon evaluation of the newly defined PBK models the models were used to translate the *in vitro* concentration response curves obtained in the hiPSC-CM-MEA assay to *in vivo* dose response curves for cardiotoxicity of ibogaine and noribogaine. To evaluate the predictions of the PBK modeling-based reverse dosimetry NAM, the predicted dose-response curves of ibogaine and noribogaine were compared to available *in vivo* data. The results obtained show that the predicted dose-response curve for ibogaine is in line with the reported QTc prolongation data especially when the reported doses were corrected for a purity of 15%, which could be considered as a representative and realistic purity of internet-purchased ibogaine as reported by Hoelen et al. (2009). It is important to note the large variation in QTc prolongation data at similar oral doses as observed in some case reports, which may be related to individuals' diverse demographic characteristics and/ or potential QTc prolonging risk factors that were not well-documented in these studies. When applicable, applying exclusion or inclusion criteria to the reported data may better illustrate the dose-dependent effects of ibogaine and thus further improve the accuracy of the evaluation. For noribogaine, the predicted dose-response curve matches well with reported dose-response curves for QTc prolongation with a difference in the $BMDL_{10}$ values derived from the predicted and reported data being less than 1.5-fold, which further demonstrates that the developed QIVIVE approach can adequately predict the *in vivo* cardiotoxicity for human.

Based on human experiences the administered dose of ibogaine for treating drug addiction has a wide range and varies from 6 to 30 mg/kg bw (equal to 420 to 2100 mg for a human of 70 kg) (Alper et al., 1999; Davis et al., 2017; Mash et al., 2018; Noller et al., 2018; Schep et al., 2016). These dose levels are 4-to 21-fold higher than our predicted $BMDL_{10}$ value (96.9 mg for a human of 70 kg) for the ibogaine dependent induction of QTc prolongation. Since a $BMDL_{10}$ value generally represents a dose level at which the adverse effect is considered negligible (EFSA, 2017), the prolonged QTc would be expected at doses higher than the predicted $BMDL_{10}$ values, which is in line with the observation that QTc prolongations and arrythmia were observed in the subjects administered dose levels of ibogaine above the predicted $BMDL_{10}$, and that a dose higher than 20 mg/kg bw ibogaine

(equal to 1400 mg for a human of 70 kg) is associated with fatalities (Mash et al., 2018). Our predictions also confirm that ECG monitoring is essential for patients receiving ibogaine (Glue et al., 2016). In addition, many studies demonstrate that ibogaine and noribogaine have different neurobiological profiles (Baumann et al., 2001a,b; Maciulaitis et al., 2008), indicating that noribogaine instead of ibogaine might be more efficient in mediating certain pharmacological effects (Mash et al., 2016). Based on our model predictions and reported observations (Glue et al., 2016), a 1.2 to 1.6 -fold higher dose of ibogaine is needed to reach the same C_{max} of noribogaine compared to the direct intake of noribogaine. Considering a similar *in vivo* potency observed in the current study for the predicted *in vivo* induction of the unwanted side effect of QTc prolongation by the two compounds (similar predicted $BMDL_{10}$ values), noribogaine would be a safer option.

In the present study we consider that a relatively small contribution of ibogaine itself to the *in vivo* cardiotoxicity could be due to its low unbound fraction in plasma and its extensive metabolism. However, as ibogaine is a basic compound, the plasma protein binding could be influenced by the level of alpha1-acid glycoprotein which has an up to 10-fold variation in human plasma (Smith and Waters, 2019). Furthermore, it has been reported that the internal concentration of ibogaine was up to 43-fold higher in CYP2D6 poor metabolizers compared to extensive metabolizers (Mash et al, 2001; Glue et al., 2015b). Glue et al. (2015b) also reported that the C_{max} of ibogaine was 26-fold higher in CYP2D6 extensive metabolizers who took CYP2D6 inhibitors compared to the ones who took placebo. Based on these observations, the cardiotoxicity of ibogaine might become apparent more easily in these sensitive individuals. Moreover, due to the limited information on the metabolism of noribogaine, only the glucuronidation was included in the current model. Other metabolic reactions such as sulfation might be also involved in the clearance of noribogaine (Glue et al., 2016). Considering the relative high potency of noribogaine in *in vivo* cardiotoxicity, it would be of interest to have a comprehensive metabolic profile for noribogaine defining also potential minor pathways for its clearance.

Based on findings in the present study, the developed in vitro-PBK modeling based approach could be extended to a higher throughput NAM for a broader range of chemicals inducing QTc prolongation, which ultimately will contribute to the use of non-animal based NAMs for human cardiac risk assessment and safety evaluations of chemicals. This can be achieved by employing a higher-throughput platform of the MEA (e.g., 96-well plate) (Kraushaar and Guenther 2019) which allows the hiPSC-CM MEA assay to be used for rapidly detecting cardiotoxicity for large numbers of chemicals. Additionally, the development of a generic PBK model which only includes a limited number and thus the most influential input parameters could accelerate the efficiency of PBK modeling, contributing to enhancing the throughput of the developed NAM. As illustrated in the present study and based on the sensitivity analysis (Text $S3^2$), such input information could include physicochemical parameters, intestinal permeability, unbound fraction in plasma and kinetic parameters for hepatic metabolic clearance. The development of high-throughput biokinetic assays to derive these parameters would further contribute to the efficiency of model parameterization

In conclusion, we demonstrated that integrating *in vitro* cardiotoxicity data obtained with hiPSC-CMs in the MEA assay, *in vitro* biokinetic data and PBK modelling can be a promising NAM to predict the *in vivo* dose-dependent cardiotoxicity of ibogaine and noribogaine in human. The comparison of the predictions obtained to the *in vivo* data indicated the adequate performance of the developed *in vitro in silico* approach. Obtained predictions also reveal that a similar *in vivo* cardiotoxicity potency upon the oral administration of ibogaine and noribogaine while noribogaine might play a substantial role in ibogaine-induced QTc prolongation. Altogether, the present study shows an additional proof of principle for using a NAM consisting of PBK modeling-based reverse dosimetry of hiPSC-CMs MEA assay data for the prediction of human cardiotoxicity, which can be used for cardiac safety evaluation.

References

Abdullah, R., Alhusainy, W., Woutersen, J. et al. (2016) Predicting points of departure for risk assessment based on in vitro cytotoxicity data and physiologically based kinetic (PBK) modeling: the case of kidney toxicity induced by aristolochic acid I. *Food and chemical toxicology* 92:104-116. doi:10.1016/j.fct.2016.03.017

Alper, K.R., Bai, R., Liu, N. et al. (2016) hERG blockade by iboga alkaloids. *Cardiovascular toxicology* 16(1):14-22. doi:10.1007/s12012-015-9311-5

Alper, K.R., Lotsof, H. S., Geerte, M. N. et al. (1999) Treatment of acute opioid withdrawal with ibogaine. *American Journal on Addictions* 8(3):234-242. doi:10.1080/105504999305848

Alper, K.R., Stajić, M., Gill, J.R. (2012) Fatalities temporally associated with the ingestion of ibogaine. *Journal of forensic sciences* 57(2):398-412. doi:10.1111/j.1556-4029.2011.02008.x

Andersen, M. E., McMullen, P.D., Phillips, M. B. et al. (2019) Developing context appropriate toxicity testing approaches using new alternative methods (NAMs). *ALTEX-Alternatives to animal experimentation* 36(4):523-534. doi:10.14573/altex.1906261

Ando, H., Yoshinaga, T., Yamamoto, W. et al. (2017) A new paradigm for drug-induced torsadogenic risk assessment using human iPS cell-derived cardiomyocytes. *Journal of pharmacological and toxicological methods* 84:111-127. doi:10.1016/j.vascn.2016.12.003

Asua, I. (2013) Growing menace of ibogaine toxicity. *British journal of anaesthesia* 111(6):1029-1030. doi:10.1093/bja/aet396

Badhan RK, Gittins R, Al Zabit D (2019) The optimization of methadone dosing whilst treating with rifampicin: a pharmacokinetic modeling study. Drug Alcohol Depend 200:168–180 doi:10.1016/j.drugalcdep.2019.03.013

Baumann, M. H., Pablo, J., Ali, S. F. et al. (2001a) Comparative neuropharmacology of ibogaine and its O-desmethyl metabolite, noribogaine. In K. Alper, G. A. Cordell (ed.) *The Alkaloids Chemistry and biology* 56 (79-113). Amsterdam, The Netherlands: Elsevier. doi:10.1016/S0099-9598(01)56009-5

Baumann, M. H., Rothman, R. B., Pablo, J. P., Mash, D. C. (2001b) In vivo neurobiological effects of ibogaine and its O-desmethyl metabolite, 12-hydroxyibogamine (noribogaine), in rats. *Journal of Pharmacology and Experimental Therapeutics* 297(2):531-539. https://pubmed.ncbi.nlm.nih.gov/11303040/

Bentz, J., O'Connor, M. P., Bednarczyk, D. et al. (2013) Variability in P-glycoprotein inhibitory potency (IC50) using various in vitro experimental systems: implications for universal digoxin drug-drug interaction risk assessment decision criteria. *Drug Metabolism and Disposition* 41(7):1347-1366. doi:10.1124/dmd.112.050500

Bos, P. M., Geraets, L., de Wit-Bos, L. et al. (2020) Towards an animal-free human health assessment: Starting from the current regulatory needs. *ALTEX-Alternatives to animal experimentation* 37(3):395-408. doi:10.14573/altex.1912041

Brown, R. P., Delp, M. D., Lindstedt, S. L. et al. (1997) Physiological parameter values for physiologically based pharmacokinetic models. *Toxicology and industrial health* 13(4):407-484. doi:10.1177/074823379701300401

Chang, Y., Fang, W. B., Lin, S. N., Moody, D. E. (2011). Stereo-selective metabolism of methadone by human liver microsomes and cDNA-expressed cytochrome P450s: a reconciliation. *Basic & clinical pharmacology & toxicology* 108(1): 55-62. doi:10.1111/j.1742-7843.2010.00628.x

Davis, A. K., Barsuglia, J. P., Windham-Herman, A. M. et al. (2017) Subjective effectiveness of ibogaine treatment for problematic opioid consumption: short-and long-term outcomes and current psychological functioning. *Journal of psychedelic studies* 1(2):65-73. doi:10.1556/2054.01.2017.009

EFSA – European Food Safety Authority (2017) Update: use of the benchmark dose approach in risk assessment. doi:10.2903/j.efsa.2017.4658

Fisher, M. B., Campanale, K., Ackermann, B. L. et al. (2000) In vitro glucuronidation using human liver microsomes and the pore-forming peptide alamethicin. *Drug metabolism and disposition* 28(5):560-566.

Florian, J., Garnett, C., Nallani, S. et al. (2012) A modeling and simulation approach to characterize methadone QT prolongation using pooled data from five clinical trials in MMT patients. *Clinical Pharmacology & Therapeutics* 91:666-672. doi:10.1038/clpt.2011.273

Foster, D. J., Somogyi, A. A., Dyer, K. R. et al. (2000) Steady-state pharmacokinetics of (R)-and (S)-methadone in methadone maintenance patients. *British journal of clinical pharmacology* 50(5):427-440. doi:10.1046/j.1365-2125.2000.00272.x

Ferruzza S., Rossi C., Sambuy, Y., Scarino M. L. (2013). Serum-reduced and serum-free media for differentiation of Caco-2 cells. ALTEX-Alternatives to animal experimentation, 30(2), 159-168. doi:10.14573/altex.2013.2.159

Gilbert-Sandoval, I., Wesseling, S., Rietjens, I. M. C. M. (2020) Predicting the Acute Liver Toxicity of Aflatoxin B1 in Rats and Humans by an In Vitro-In Silico Testing Strategy. *Molecular nutrition & food research* 64(13):2000063. doi:10.1002/mnfr.202000063

Glue, P., Cape, G., Tunnicliff, D. et al. (2016) Ascending single-dose, double-blind, placebo-controlled safety study of noribogaine in opioid-dependent patients. *Clinical pharmacology in drug development* 5(6):460-468. doi:10.1002/cpdd.254

Glue, P., Lockhart, M., Lam, F. et al. (2015a) Ascending-dose study of noribogaine in healthy volunteers: Pharmacokinetics, pharmacodynamics, safety, and tolerability. *The Journal of Clinical Pharmacology* 55(2):189-194. doi:10.1002/jcph.404

Glue, P., Winter, H., Garbe, K. et al. (2015b) Influence of CYP2D6 activity on the pharmacokinetics and pharmacodynamics of a single 20 mg dose of ibogaine in healthy volunteers. *The Journal of Clinical Pharmacology* 55(6):680-687. doi:10.1002/jcph.471

Goutarel, R., Gollnhofer, O., Sillans, R. (1993) Pharmacodynamics and therapeutic applications of iboga and ibogaine. *Psychedelic Monographs and Essays* 6 (71-111) https://ibogainedossier.com/bwiti1.html

Grogan, J., Gerona, R., Snow, J. W., Kao, L. (2019) Ibogaine Consumption With Seizure-Like Episodes, QTc-Prolongation, and Captured Cardiac Dysrhythmias. *The Journal of emergency medicine* 57(4):e99-e104. doi:10.1016/j.jemermed.2019.06.05

Henstra, M., Wong, L., Chahbouni, A., Swart, N. et al. (2017) Toxicokinetics of ibogaine and noribogaine in a patient with prolonged multiple cardiac arrhythmias after ingestion of internet purchased ibogaine. *Clinical Toxicology* 55(6):600-602. doi:10.1080/15563650.2017.1287372

Hildyard, C., Macklin, P., Prendergast, B., Bashir, Y. (2016) A case of QT prolongation and torsades de pointes caused by ibogaine toxicity. *Journal of Emergency Medicine* 50(2):e83-e87. doi:10.1016/j.jemermed.2015.06.05

Hoelen, D. W., Spiering, W., Valk, G. D. (2009) Long-QT syndrome induced by the antiaddiction drug ibogaine. *New England journal of medicine* 360(3):308-309. doi:10.1056/NEJMc0804248

Hubatsch, I., Ragnarsson, E. G., Artursson, P. (2007) Determination of drug permeability and prediction of drug absorption in Caco-2 monolayers. *Nature protocols* 2(9):2111. doi:10.1038/nprot.2007.303

ICCVAM – Interagency Coordinating Committee on the Validation of Alternative Methods (2018). A Strategic Roadmap for Establishing New Approaches to Evaluate the Safety of Chemicals and Medical Products in the United States. doi:10.22427/NTP-ICCVAM-ROADMAP2018.

ICH – The International Council for Harmonisation of Technical Requirements for Pharmaceuticals for Human Use (2005) E14: the clinical evaluation of QT/QTc interval prolongation and proarrhythmic potential for non-antiarrhythmic drugs. https://database.ich.org/sites/default/files/E14_Guideline.pdf Accessed 20 Jan 2021

Karakikes, I., Ameen, M., Termglinchan, V., Wu, J. C. (2015) Human induced pluripotent stem cell-derived cardiomyocytes: insights into molecular, cellular, and functional phenotypes. *Circulation research* 117(1):80-88. doi:10.1161/CIRCRESAHA.117.305365

Kitaguchi, T., Moriyama, Y., Taniguchi, T. et al. (2017) CSAHi study: detection of drug-induced ion channel/receptor responses, QT prolongation, and arrhythmia using multi-electrode arrays in combination with human induced pluripotent stem cell-derived cardiomyocytes. *Journal of pharmacological and toxicological methods* 85:73-81. doi:10.1016/j.vascn.2017.02.001

Koenig, X., Kovar, M., Boehm, S. et al. (2014) Anti-addiction drug ibogaine inhibits hERG channels: a cardiac arrhythmia risk. Addiction biology 19(2):237-239. doi:10.1111/j.1369-1600.2012.00447.x

Kraushaar U, Guenther E (2019) Assay procedures for compound testing of hiPSC-derived cardiomyocytes using multiwell microelectrode arrays Cell-Based Assays Using iPSCs for Drug Development and Testing. Springer, p 197-208. doi:10.1007/978-1-4939-9477-9_18

Kussauer, S., David, R., Lemcke, H. (2019) hiPSCs derived cardiac cells for drug and toxicity screening and disease modeling: what micro-electrode-array analyses can tell us. *Cells* 8(11):1331. doi:10.3390/cells8111331

Litjens, R. P., Brunt, T. M. (2016) How toxic is ibogaine? *Clinical Toxicology* 54(4):297-302. doi:10.3109/15563650.2016.1138226

Louisse, J., de Jong, E., van de Sandt, J. J. et al. (2010) The use of in vitro toxicity data and physiologically based kinetic modeling to predict dose-response curves for in vivo developmental toxicity of glycol ethers in rat and man. *Toxicological Sciences* 118(2):470-484. doi:10.1093/toxsci/kfq270

Ma, J., Guo, L., Fiene, S. J. et al. (2011) High purity human-induced pluripotent stem cell-derived cardiomyocytes: electrophysiological properties of action potentials and ionic currents. *American Journal of Physiology-Heart and Circulatory Physiology* 301(5):H2006-H2017. doi:10.1152/ajpheart.00694.2011

Maciulaitis, R., Kontrimaviciute, V., Bressolle, F., Briedis, V. (2008) Ibogaine, an anti-addictive drug: pharmacology and time to go further in development. A narrative review. *Human and Experimental Toxicology* 27(3):181. doi:10.1177/0960327107087802

Martin, R. L., McDermott, J. S., Salmen, H. J. et al. (2004) The utility of hERG and repolarization assays in evaluating delayed cardiac repolarization: influence of multi-channel block. *Journal of cardiovascular pharmacology* 43(3):369-379. doi:10.1097/00005344-200403000-00007

Mash, D. C., Kovera, C. A., Pablo, J. et al. (2001). Ibogaine in the treatment of heroin withdrawal. *The Alkaloids Chemistry and biology* 56 (155-171). Amsterdam, The Netherlands: Elsevier. doi:10.1016/S0099-9598(01)56012-5

Mash, D. C., Ameer, B., Prou, D. et al. (2016) Oral noribogaine shows high brain uptake and anti-withdrawal effects not associated with place preference in rodents. *Journal of Psychopharmacology* 30(7):688-697. doi:10.1177/0269881116641331

Mash, D. C., Duque, L., Page, B., Allen-Ferdinand. K. (2018) Ibogaine detoxification transitions opioid and cocaine abusers between dependence and abstinence: clinical observations and treatment outcomes. *Frontiers in pharmacology* 9:529. doi:10.3389/fphar.2018.00529

Meisner, J. A., Wilcox, S. R., Richards, J. B. (2016) Ibogaine-associated cardiac arrest and death: case report and review of the literature. *Therapeutic advances in psychopharmacology* 6(2):95-98. doi:10.1177/2045125315626073

Mujtaba, S., Romero, J., Taub, C. C. (2013) Methadone, QTc prolongation and torsades de pointes: current concepts, management and a hidden twist in the tale? *Journal of Cardiovascular Disease Research* 4:229-235. doi:10.1016/j.jcdr.2013.10.001

Ning, J., Louisse, J., Spenkelink, B. et al. (2017) Study on inter-ethnic human differences in bioactivation and detoxification of estragole using physiologically based kinetic modeling. *Archives of toxicology* 91(9):3093-3108. doi:10.1007/s00204-017-1941-x

Noller, G. E, Frampton, C. M., Yazar-Klosinski, B. (2018) Ibogaine treatment outcomes for opioid dependence from a twelve-month follow-up observational study. *The American journal of drug and alcohol abuse* 44(1):37-46. doi:10.1080/00952990.2017.1310218

Nozaki, Y., Honda, Y., Watanabe, H. et al. (2017) CSAHi study-2: validation of multi-electrode array systems (MEA60/2100) for prediction of drug-induced proarrhythmia using human iPS cell-derived cardiomyocytes: assessment of reference compounds and comparison with non-clinical studies and clinical information. *Regulatory Toxicology and Pharmacology* 88:238-251. doi:10.1016/j.yrtph.2017.06.006

O'Connell, C. W., Gerona, R. R, Friesen, M. W, Ly, B. T. (2015) Internet-purchased ibogaine toxicity confirmed with serum, urine, and product content levels. *The American journal of emergency medicine* 33(7):985. e5-985. e6. doi:10.1016/j.ajem.2014.12.023

Obach, R. S, Pablo, J., Mash, D. C. (1998) Cytochrome P4502D6 catalyzes the O-demethylation of the psychoactive alkaloid ibogaine to 12-hydroxyibogamine. *Drug metabolism and disposition* 26(8):764-768.

Ovics, P., Regev, D., Baskin, P. et al. (2020) Drug Development and the Use of Induced Pluripotent Stem Cell-Derived Cardiomyocytes for Disease Modeling and Drug Toxicity Screening. *International Journal of Molecular Sciences* 21(19):7320. doi:10.3390/ijms21197320

Paling, F., Andrews, L., Valk, G., Blom, H. (2012) Life-threatening complications of ibogaine: three case reports. *The Netherlands Journal of Medicine* 70(9):422-4.

Pang, L., Sager, P., Yang, X. et al. (2019) Workshop report: FDA workshop on improving cardiotoxicity assessment with human-relevant platforms. *Circulation research* 125(9):855-867. doi:10.1161/CIRCRESAHA.119.315378

Patterson, E. A., Whelan, M. P., Worth, A. P. (2020) The role of validation in establishing the scientific credibility of predictive toxicology approaches intended for regulatory application. *Computational Toxicology*:100144. doi:10.1016/j.comtox.2020.100144

Pleskovic, A., Gorjup, V., Brvar, M., Kozelj, G. (2012) Ibogaine-associated ventricular tachyarrhythmias. *Clinical Toxicology* 50 (2): 157-157. doi:10.3109/15563650.2011.647031

Punt, A., Bouwmeester, H., Blaauboer, B. J. et al. (2020) New approach methodologies (NAMs) for human-relevant biokinetics predictions: Meeting the paradigm shift in toxicology towards an animal-free chemical risk assessment. *ALTEX-Alternatives to animal experimentation* 37(4):607-622. doi:10.14573/altex.2003242

Rietjens, I. M. C. M., Louisse, J., Punt, A. (2011) Tutorial on physiologically based kinetic modeling in molecular nutrition and food research. *Molecular nutrition & food research* 55(6):941-956. doi:10.1002/mnfr.201000655

Rohatgi, A. (2020). WebPlotDigitizer (Version 4.4) [Computer software]. Retrieved from https://apps.automeris.io/wpd/

Rubi, L., Eckert, D., Boehm, S. et al. (2017) Anti-addiction drug ibogaine prolongs the action potential in human induced pluripotent stem cell-derived cardiomyocytes. *Cardiovascular toxicology* 17(2):215-218. doi:10.1007/s12012-016-9366-y

Sala, L., Ward-van Oostwaard, D., Tertoolen, L. G. et al. (2017) Electrophysiological analysis of human pluripotent stem cell-derived cardiomyocytes (hPSC-CMs) using multi-electrode arrays (MEAs). *JoVE (Journal of Visualized Experiments)*(123):e55587. doi:10.3791/55587

Satsuka, A., Kanda, Y. (2020) Cardiotoxicity Assessment of Drugs Using Human iPS Cell-Derived Cardiomyocytes: Toward Proarrhythmic Risk and Cardio-Oncology. *Current pharmaceutical biotechnology* 21(9):765-772. doi:10.2174/1389201020666190628143345

Schep, L. J., Slaughter, R., Galea, S., Newcombe, D. (2016) Ibogaine for treating drug dependence. What is a safe dose? *Drug and alcohol dependence* 166:1-5. doi:10.1016/j.drugalcdep.2016.07.005

Shi, M., Bouwmeester, H., Rietjens, I. M. C. M., Strikwold, M. (2020a) Integrating in vitro data and physiologically based kinetic modeling-facilitated reverse dosimetry to predict human cardiotoxicity of methadone. *Archives of toxicology* 94(8):2809-2827. doi:10.1007/s00204-020-02766-7

Shi, M., Tien, N. T., de Haan, L. et al. (2020b). Evaluation of in vitro models of stem cell-derived cardiomyocytes to screen for potential cardiotoxicity of chemicals. *Toxicology in Vitro*: 104891. doi:10.1016/j.tiv.2020.104891

Smith, D. A., Di, L., Kerns, E. H. (2010) The effect of plasma protein binding on in vivo efficacy: misconceptions in drug discovery. *Nature reviews Drug discovery* 9(12):929-939. doi:10.1038/nrd3287

Smith, S. A., Waters, N. J. (2019) Pharmacokinetic and pharmacodynamic considerations for drugs binding to alpha-1-acid glycoprotein. *Pharmaceutical research* 36(2):1-19. doi:10.1007/s11095-018-2551-x

Steinberg, C., Deyell, M. W. (2018) Cardiac arrest after ibogaine intoxication. *Journal of arrhythmia* 34(4):455-457. doi:10.1002/joa3.12061

Strikwold, M., Spenkelink, B., de Haan, L. et al. (2017) Integrating in vitro data and physiologically based kinetic (PBK) modelling to assess the in vivo potential developmental toxicity of a series of phenols. *Archives of toxicology* 91(5):2119-2133. doi:10.1007/s00204-016-1881-x

Taboureau, O., El M'Selmi, W., Audouze, K. (2020) Integrative systems toxicology to predict human biological systems affected by exposure to environmental chemicals. *Toxicology and Applied Pharmacology* 405:115210. doi:10.1016/j.taap.2020.115210

van Liempd, S., Morrison, D., Sysmans, L. et al. (2011) Development and validation of a higher-throughput equilibrium dialysis assay for plasma protein binding. *JALA: Journal of the Association for Laboratory Automation* 16(1):56-67. doi:10.1016/j.jala.2010.06.002

Vandenberk B, Vandael E, Robyns T, et al. (2016) Which QT correction formulae to use for QT monitoring? *Journal of the American Heart Association* 5(6):e003264. doi:10.1161/JAHA.116.003264

Vlaanderen, L., Martial, L., Franssen, E. et al. (2014) Cardiac arrest after ibogaine ingestion. *Clinical Toxicology* 52(6):642-643. doi:10.3109/15563650.2014.927477

Waters, N. J., Jones, R., Williams, G., Sohal, B. (2008) Validation of a rapid equilibrium dialysis approach for the measurement of plasma protein binding. *Journal of pharmaceutical sciences* 97(10):4586-4595. doi:10.1002/jps.21317

Wedam, E. F., Bigelow, G. E., Johnson, R. E. et al. (2007) QT-interval effects of methadone, levomethadyl, and buprenorphine in a randomized trial. *Archives of Internal Medicine* 167:2469-2475. doi:10.1001/archinte.167.22.2469

Wolff, K., Rostami-Hodjegan, A., Hay, A. et al. (2000) Population-based pharmacokinetic approach for methadone monitoring of opiate addicts: potential clinical utility. *Addiction* 95(12):1771-1783. doi:10.1046/j.1360-0443.2000.951217717.x

World Health Organization (WHO). (2010). Characterization and application of physiologically based pharmacokinetic models in risk assessment. https://www.inchem.org/documents/harmproj/ harmproj/harmproj9.pdf.

Zhao, S., Kamelia, L., Boonpawa, R. et al. (2019) Physiologically based kinetic modeling-facilitated reverse dosimetry to predict in vivo red blood cell acetylcholinesterase inhibition following exposure to chlorpyrifos in the Caucasian and Chinese population. *Toxicological sciences* 171(1):69-83. doi:10.1093/toxsci/kfz134

Zwartsen, A., de Korte, T., Nacken, P. et al. (2019) Cardiotoxicity screening of illicit drugs and new psychoactive substances (NPS) in human iPSC-derived cardiomyocytes using microelectrode array (MEA) recordings. *Journal of molecular and cellular cardiology* 136:102-112. doi:10.1016/j.yjmcc.2019.09.007

Conflict of interest

All authors declare that they have no conflict of interest.

Acknowledgements

This work was funded by a Grant from the China Scholarship Council (No. 201607720029).